

How to Train PointGoal Navigation Agents on a (Sample and Compute) Budget

Erik Wijmans^{1,2}, Irfan Essa^{1,3}, and Dhruv Batra^{2,1}

¹Georgia Institute of Technology, ²Facebook AI Research, ³Google Research Atlanta
{etw, irfan, dbatra}@gatech.edu

Abstract

PointGoal Navigation has seen significant recent interest and progress, spurred on by the Habitat platform and associated challenge [1]. In this paper, we study PointGoal Navigation under both a sample budget (75 million frames) and a compute budget (1 GPU for 1 day). We conduct an extensive set of experiments, cumulatively totaling over 50,000 GPU-hours, that let us identify and discuss a number of ostensibly minor but significant design choices – the advantage estimation procedure (a key component in training), visual encoder architecture, and a seemingly minor hyper-parameter change. Overall, these design choices lead to considerable and consistent improvements over the baselines present in Savva et al. [1]. Under a sample budget, performance for RGB-D agents improves 8 SPL on Gibson (14% relative improvement) and 20 SPL on Matterport3D (38% relative improvement). Under a compute budget, performance for RGB-D agents improves by 19 SPL on Gibson (32% relative improvement) and 35 SPL on Matterport3D (220% relative improvement). We hope our findings and recommendations will make serve to make the community’s experiments more efficient.

1. Introduction

Galvanized by fast simulation platforms [1, 2, 3], large rich 3D datasets [4, 5, 6], and the success of deep reinforcement learning [7, 8, 9], training virtual robots (embodied agents) in simulation has garnered considerable interest in recent years. Works have developed a rich set of tasks, ranging from PointGoal Navigation [10], to grounded instruction following [11, 12] and question answering [13, 14, 15].

In this rich space of tasks, PointGoal Navigation with GPS+Compass has emerged as a test-bed problem due to its property of ‘easy to get off the ground, but difficult to fully solve’. Specifically, Wijmans *et al.* [16] show that good performance can be obtained with under a week of GPU time but near-perfect performances currently requires *half-a-year* of GPU time. Moreover, findings and improvements

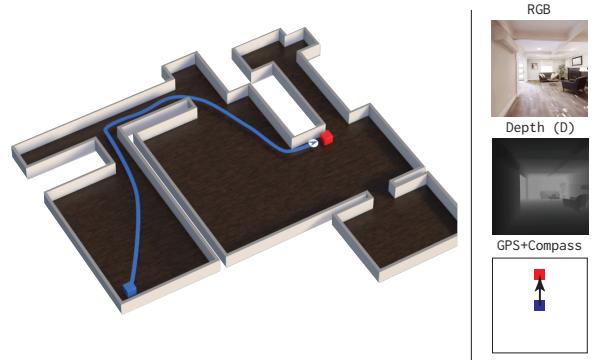


Figure 1: **PointGoal Navigation** [10]. An agent is initialized in a novel environment (blue square) and task with navigation to a point specified relative to the start location (red square) – e.g. (5, 2) means go 5 meters forward and 2 meters right. It must do so from egocentric inputs – RGB-D and GPS+Compass– and without a map.

in PointGoalNav with GPS+Compass generally translate to other tasks (PointGoalNav without GPS+Compass [17, 18], ObjectGoal navigation [19, 20], RoomGoal navigation [21]) and to navigation by real robots [22].

Given this interest, we present a systematic analysis of what matters and what doesn’t matter for learning PointGoalNav with GPS+Compass on a limited sample or compute budget. We identify and discuss a number of ostensibly minor but significant design choices – the advantage estimation procedure (a key component in training), visual encoder architecture, and a hyper-parameter change – that have large impacts on agent performance.

We examine these differences in two contexts, i) *sample* efficiency, and ii) *compute* efficiency. To study sample efficiency, we train all agent variants for a fixed number of samples – 75 million steps as represents a high but feasible number of samples [1, 23, 24, 25, 26]. To study compute efficiency, we ask a subtly different but important question: *How far can we get with 1 GPU for 1 day?* Instead of training for a fixed number of samples, we train

for a fixed amount of computation – *i.e.* comparisons at a different number of samples but the same amount of computation.

Specifically, we contend that when that when training in simulation compute efficiency should be an equally important objective. For instance, an agent architecture or training regime that *increases* the number of samples required 2-fold but *decreases* the compute required 6-fold would be desirable when training in simulation. On the other hand, an architecture or training regime that *reduces* the number of samples required 2-fold but *increases* the compute required 6-fold would not be desirable.

Under these two objectives, we conduct an extensive set of experiments, cumulatively totalling over 50,000 GPU hours, and draw the following findings:

- **Visual Encoder.** Relatively small CNNs are common place in visual navigation [27, 28, 25, 29, 6]. We examine using a moderately deep CNN (ResNet18 [30]) as Wijmans *et al.* [16] used a very deep to ‘solve’ the task. We find that ResNet18 improves the sample efficiency of all agent variants and improve the compute efficiency of most – it only harms the compute efficiency of Depth-only agents. ResNet18’s improvements to sample efficiency outweigh its increased compute for RGB-D agents and considerably for RGB agents.
- **Advantage Estimation.** Batch-wise normalizing advantage (a key component in policy optimization) is a common place ‘code-level’ optimization [31] for advantage actor-critic methods however it is rarely discussed in the literature. We present a systematic and controlled study of it in multi-environment goal-conditioned reinforcement learning. For the simple 3-layer CNN agents, we find it harms performance. For the ResNet18 agents, we find it provides little to no benefit and it can make training unstable. Given this, we recommend not batch-wise normalizing advantage.
- **Mini-Batch Size.** We perform systematic experiments to examine the impact of learning mini-batch size and that large batches (*i.e.* containing over 300 transitions) improves both the sample efficiency and compute efficiency for *all* agent variants studied.

These design choices to lead considerable and consistent improvements. Under a fixed sample budget, performance for RGB-D agents improves over the Habitat baselines by 8 SPL on Gibson (14% relative improvement) and 20 SPL on Matterport3D (38% relative improvement). Under a fixed compute budget (1 GPU-day), performance for RGB-D agents improves by 19 SPL on Gibson (32% relative improvement) and 35 SPL on Matterport3D (220% relative improvement). We hope our findings and recommendations will make serve to make the community’s experiments more efficient.

2. Related Work

Visual Navigation. Training virtual robots for visual navigation has been a subject of much interest in recent years [13, 15, 11, 14]. In this space, PointGoal Navigation has seen considerable interest recently with works proposing to leverage hierarchical models [24], pre-trained representations [25, 28], auxiliary-tasks [23], or distribution and very deep networks [16] to improve performance and/or sample efficiency.

Sample efficiency in model-free reinforcement learning (RL). Sample efficiency has been studied extensively in model-free RL, with works proposing new training methods [32, 33], auxiliary losses [34, 35, 36], intrinsic rewards [37], pre-training [25], and data-augmentation [38, 39] to improve sample efficiency. In comparison, we study how ostensibly minor changes impact sample efficiency and find they can have profound impacts.

Compute efficiency in model-free RL. Compute efficiency has been studied in model-free RL in the context of distributed systems methods [16, 40, 41, 42]. We study compute efficiency with less compute (1 GPU for 1 day) and instead study changes to architecture or hyper-parameters.

Systematic studies of RL. Closely related to our work is that of [31], who present systematic studies of how ‘code-level’ optimizations impact perform for on-policy RL in Atari. Concurrently, [43] present a systematic study of the impact of a wide variety of techniques on on-policy RL in DeepMind Control. Of particular relevance to our work, they find mixed results batch-normalizing advantage. We find this technique to often be harmful and their result helps to confirm that normalized advantage may not be necessary in general. These works both perform their study in single-environment single-goal reinforcement learning problems (Atari and DeepMind Control). We instead multi-environment (*i.e.* agents trained in multiple houses) goal-conditioned (*i.e.* agents trained to navigate to a provided goal) reinforcement learning, to the best of our knowledge this is the first such study.

3. Task, Agent, and Training on a Sample Budget

The starting point for our study is Savva *et al.* [1] and Wijmans *et al.* [16], who both presented large advances in training agents for PointGoal Navigation– the former showing that learned policies can outperform classical method and the latter showing that learned policies can ‘solve’ this task when trained for 2.5 billion samples. In this section we discuss their similarities and differences in task, agent, and training procedure.

PointGoal Navigation (PointGoalNav). Savva *et al.* [1]; Wijmans *et al.* [16] train and evaluate agents for PointGoalNav [10] utilizing the AI Habitat platform [1]. In PointGoalNav the agent is initialized at a random lo-

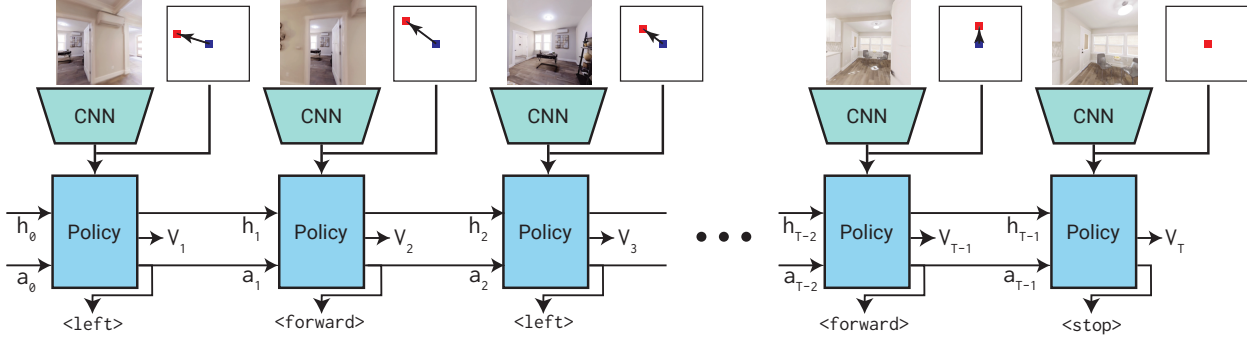


Figure 2: **Agent Architecture.** The architecture consists of two components, a visual encoder (parametrized by a CNN) and a policy (parametrized by an RNN). At every timestep, the agent receives visual observations (e.g. RGB or RGB-D), use its GPS+Compass sensor to update the goal coordinates to be relative to its current location, and then predicts an action. We compare the SimpleCNN agent from [1] and the ResNet [30] agent from Wijmans *et al.* [16].

cation in a previously unseen environment and then tasked with navigating to a point specified relative to the starting location – e.g. $(\delta x, \delta y)$ means go δx meters forwards and δy meters right. As shown in Fig. 1, the agent is equipped with RGB camera, a Depth sensor (or their combinations, {RGB, Depth, RGB-D}) – providing 256x256 ego-centric color and/or depth observations at every time-step – and a GPS+Compass sensor – providing position and orientation relative to the starting location at every time-step.

The agent has 4 primitive actions – move_forward (0.25m), turn_right/turn_left (10°), and stop. Performance is analyzed by two metrics – 1) Success, whether or not the agent took stop within 0.2m of the goal, and 2) Success weighted by (normalized inverse) Path Length (SPL) [10] – a measure of success and efficiency. Agents are trained and evaluated in either the (a) Matterport3D (MP3D) dataset [5] – comprised of 61/11 training/validation scenes – or (b) [1]’s curation of the Gibson dataset [6] – containing 72/14 training/validation scenes.

Agent designs. Savva *et al.* [1]; Wijmans *et al.* [16] employ similar agent architectures, shown in Fig. 2 – the agent is divided into a visual encoder and policy, and utilizes its GPS+Compass sensor to update the goal location to be relative to current location. In [1], the visual observation (e.g. RGB) is encoded by a 3-layer CNN (SimpleCNN) and then concatenated with the goal (relative to current location) in polar coordinates $([r, \theta])$. The policy (a 1-layer GRU and a linear layer) then produces a softmax distribution over the action space and estimate of the value function.

Wijmans *et al.* [16] instead use a large CNN (e.g. ResNet50 [30]) to produce an embedding of the visual observation. This is concatenated with a learnable embedding of the previous action taken and a learnable embedding of the goal. Given the goal in polar coordinates $[r, \theta]$, the goal is first transformed to $[r, \cos(\theta), \sin(\theta)]$ and then projected to 32-d with a learned matrix to 1) handle the discontinu-

ity at 180 degrees and 2) allow the agent to learn whatever normalization is sensible. The policy is a 2-layer LSTM followed by a linear layer. We change the 2-layer LSTM to a 1-layer GRU (matching the SimpleCNN agent) and use ResNet18 as the backbone visual encoder to reduce training time. Further, plots in Wijmans *et al.* [16] show that the deeper CNNs are improve final performance but do not influence initial performance. We follow the same procedure as Wijmans *et al.* [16] to adapt ResNet18 – reduce the number of output channels by half, add an initial 2×2 -AvgPool, replace BatchNorm with GroupNorm [44], and replace the final global average pool with 3×3 -Conv+Flatten to produce a 2048-d vector. As in Wijmans *et al.* [16], for the RGB and RGB-D agents, we normalize the visual inputs (subtract/divide by running-across-episodes mean/standard deviation).

Advantage Estimation and Reward. One subtle difference between the training procedures is how advantage (a key component in PPO) is estimated. While both Savva *et al.* [1]; Wijmans *et al.* [16] use GAE, Savva *et al.* [1] employ an additional trick known as normalized advantage – the estimated advantages are normalized to have zero mean and unit variance per batch. This is particularly important because this trick falls under the realm of ‘code-level optimizations’ [31] and is not described in any papers using it, to the best of our knowledge. While it is common place, effective, and (possibly) sensible single-environment single-goal settings, *i.e.* Atari, it is unclear if this transfers to the multi-environment goal-conditioned setting of Habitat. Wijmans *et al.* [16] found this to introduce instabilities at their scale and did not use it. We conduct systematic experiments to study its affect while controlling for others factors.

Savva *et al.* [1]; Wijmans *et al.* [16] use the same general reward structure. Let s_t be the agent’s state at time t and a_t be the action taken, then reward is

#	Sensors	Norm Adv.	HyperParams	SimpleCNN				ResNet18			
				Gibson		Matterport3D		Gibson		Matterport3D	
				Success \uparrow	SPL \uparrow						
1*		✓	Set 1	72	54	-	~28	-	-	-	-
1	RGB	✓	Set 1	69.2±2.52	53.9±1.39	34.8±2.79	25.2±1.76	71.6±1.92	60.1±1.99	46.5±0.78	33.8±1.23
2		-	Set 1	75.3±1.67	57.5±2.00	34.2±2.81	25.4±2.44	79.6±1.32	65.4±1.10	46.8±3.21	35.7±0.92
3		✓	Set 2	14.2±24.97	11.2±19.56	00.0±0.00	00.0±0.00	79.3±1.57	68.0±1.26	53.1±2.03	40.1±0.86
4		-	Set 2	78.5±2.20	63.2±1.76	55.1±3.28	37.6±1.77	81.8±2.14	68.4±1.38	50.8±1.46	37.9±1.40
5*		✓	Set 1	78	69	-	~42	-	-	-	-
5	RGB-D	✓	Set 1	79.8±0.67	70.1±1.32	62.0±2.80	46.8±2.10	87.0±1.15	78.7±1.62	73.3±1.03	58.1±1.39
6		-	Set 1	84.4±0.75	73.5±0.67	71.4±0.94	54.8±2.39	87.2±0.73	77.3±0.37	74.6±2.23	60.6±1.49
7		✓	Set 2	85.1±1.29	77.4±1.32	55.5±31.39	45.9±26.00	87.4±0.75	80.5±0.77	78.8±1.02	66.7±1.07
8		-	Set 2	87.3±1.39	78.0±0.79	75.2±2.56	60.9±1.82	88.6±0.80	80.3±0.36	78.3±0.98	64.7±1.05
9*		✓	Set 1	86	78	-	~55	-	-	-	-
9	Depth	✓	Set 1	85.2±1.99	74.8±3.23	70.5±1.20	57.0±0.79	89.9±1.85	80.6±1.98	76.0±1.37	62.3±1.44
10		-	Set 1	87.4±1.79	77.6±1.35	75.7±0.99	61.8±1.16	91.3±0.75	80.8±0.49	77.5±1.75	63.2±1.01
11		✓	Set 2	88.6±1.67	81.9±0.93	78.3±0.29	65.9±0.50	91.8±1.35	83.9±0.58	81.8±1.17	69.3±1.49
12		-	Set 2	93.1±0.59	84.4±0.44	80.1±1.42	66.5±1.14	93.0±0.57	84.2±0.55	80.5±1.79	66.9±0.97

Table 1: **Results on PointGoalNav at 75 million.** Performance reported on the Gibson and Matterport3D validation sets (validation used to reduce exposure to test). Checkpoint selection done by validation SPL for each run independently. * denotes the results from [1] for reference – Matterport3D numbers taken from plots (and thus approximate), Gibson numbers from re-evaluation of released model weights. We find that ResNet18 improves performance and normalized advantage can harm performance. We also find that relatively minor changes in hyper-parameters results in large changes for SimpleCNN while ResNet18 without normalized advantage is more consistent. Mean and 95% CI from 5 runs.

$$r(s_t, a_t) = \begin{cases} \beta \cdot \text{Success} & \text{if } a_t = \text{stop} \\ -\Delta_{\text{GeoDist}}(s_t, a_t) - \lambda & \text{otherwise} \end{cases} \quad (1)$$

where $\Delta_{\text{GeoDist}}(s_t, a_t)$ is the change in geodesic distance to goal and $\lambda(=0.01)$ is a slack penalty.¹ [1] set $\beta=10.0$ and Wijmans *et al.* [16] set $\beta=2.5$ (no normalized advantage).

Training. Savva *et al.* [1]; Wijmans *et al.* [16] use Proximal Policy Optimization (PPO) [32] with Generalized Advantage Estimation (GAE) [45]. Following [1] we set utilize discount factor $\gamma=0.99$, GAE $\tau=0.95$, a rollout length of 128, and a learning rate of 2.5×10^{-4} . We linearly decay the learning rate and PPO clip ϵ to 1/3rd of their initial values over the course of training. For each PPO update, we collect 128×6 steps of experience from 6 parallel instances of the simulator (all the same GPU and each with a different scene). Recently, Habitat add support for texture compressed MP3D meshes. These texture compressed meshes use $4 \times 6 \times$ less GPU memory (*e.g.* a reduction from 4GB to 700 MB) With these, we are able to train agents on a *single* 12GB Titan XP compared to the 4-GPU setup used in [1] where 3 GPUs were used for rendering.

We consider two different settings for the PPO clip ϵ and the number of mini-batches per PPO epoch.

¹Wijmans *et al.* [16] weight the terminal reward by SPL. We omit this for consistency and as it isn’t influential at this scale of training.

	Set 1	Set 2
PPO Clip (ϵ)	0.1	0.2
Mini-batches per epoch	6 ²	2

Set 1 replicates the Matterport3D hyper-parameters from [1] exactly. Set 2 results in hyper-parameters that are nearly identical to Wijmans *et al.* [16]. The only difference is 4 PPO epochs instead of 2 as [1] used 4. We use the same number of PPO epochs for both hyper-parameter sets to isolate the effect of changing how many times a given step of experience is used to update the model.³

We train agents under either a sample budget or compute budget. Under a sample budget, we match [1] and use 75 million frames of experience. Under a compute budget, we use 1-GPU day (discussed further in Sec. 5)

Evaluation Protocol. Agents are evaluated on held out scenes from the validation set. We do not use the test set to avoid over-fitting to the test-set. During evaluation, the agent must navigate solely from its egocentric sensor (*i.e.* RGB-D and GPS+Compass) and reward is not given.

4. Results on a Sample Budget

In this section we discuss our results when considering *sample* efficiency. Tab. 1 shows our results. The rows

²This was reported as 4 in [1], however, we confirmed with the authors and the implementation results in 6 for MP3D and 4 for Gibson. We use their MP3D hyper-parameters on both MP3D and Gibson.

³We do not ablate 2 vs. 4 epochs to reduce the size of the grid. The current grid required 240 agents and 40,000 GPU hours.

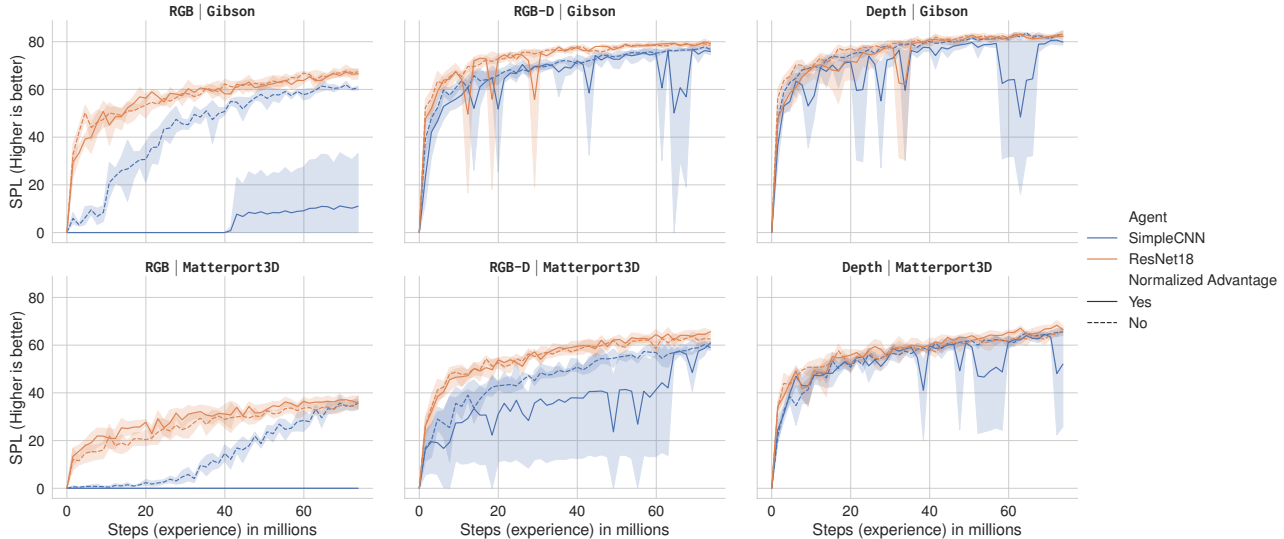


Figure 3: **Performance (SPL; higher is better)** using hyper-parameter set 2 as a function of experience. Note the spurious dips in performance for the variants with normalize advantage. Shading represents 95% CI drawn over 5 runs.

show the 12 different agent settings studied – $\{\text{RGB, RGB-D, Depth}\} \times \{\text{Hyper-Parameter Set 1, Hyper-Parameter Set 2}\} \times \{\text{normalized advantage, unnormalized advantage}\}$. The columns show the 4 different settings each agent is trained under – $\{\text{Gibson, Matterport3D}\} \times \{\text{SimpleCNN, ResNet18}\}$. We focus our analysis on hyper-parameter set 1 initially and then discuss hyper-parameter set 2. We refer to changes in performance as $\{+,-\}X/\{+,-\}Y$ SPL to indicate an $\{\text{increase, decrease}\}$ of X SPL on Gibson and a $\{\text{increase, decrease}\}$ of Y SPL on Matterport3D.

Normalized advantage harms performance (for SimpleCNN). We find that normalized advantage harms performance for SimpleCNN in almost all cases and *never* improves performance – $+6/+0$ SPL for RGB (row 2 vs. 1), $+3/+8$ SPL for RGB-D (6 vs. 5), and $+3/+5$ SPL for Depth (10 vs. 9). For ResNet18, normalized advantage neither harms nor improves the performance of the best checkpoint by a statically significant margin. For both, normalized advantage introduces instability – *i.e.* agent performance will spuriously collapse before recovering shortly (see RGB-D |Gibson in Fig. 3). Despite its prevalence, we find clear evidence that this method is harmful.

ResNet18 improves performance. The largest visible difference between Savva *et al.* [1] and Wijmans *et al.* [16] is the choice of visual encoder. Savva *et al.* [1] use a simple 3-layer CNN that has its origins in Atari experiments [46] and contains none of the features of modern CNNs – *e.g.* no skip-connections [30] nor normalization layers [47]. Due to the visual complexity of Gibson and Matterport, a better CNN improves performance considerably – $+8/+10$ SPL for RGB (row 1), $+4/+5$ SPL for RGB-D (row 6), and $+3/+0$ SPL

for Depth (row 10). As we transition from RGB to RGB-D to Depth, the improvements due to ResNet18 decrease, indicating that Depth is already a highly conducive visual representation for PointGoalNav with GPS+Compass.

The gap between RGB-D and Depth closes. One intriguing trend of Savva *et al.* [1] is the difference in performance between the RGB-D and Depth agents, particularly on Matterport3D (gap of 13 SPL, row 5* vs. 9*, left). The RGB-D agent could clearly do better if it simply ignored RGB but instead fails to learn to do so. We find that given a better visual encoder, this gap closes considerably, to 2 SPL (row 6 vs. 10, right). Specifically, the RGB-D performance on Matterport3D with ResNet18 and no normalized advantage is 61 SPL, while the performance with Depth is 63 SPL.

Hyper-parameter set 2 improves performance further. For ResNet18 agents, the relatively minor change to hyper-parameter set 2 improves SPL by at least 3 in all cases. Interesting, we find that SimpleCNN benefits more than ResNet18 from hyper-parameter set 2. For Depth, SimpleCNN nearly matches the performance of the ResNet18 agent, indicating that Depth-only is an powerful inductive basis for PointGoalNav with GPS+Compass.

5. Training on a Compute Budget

We re-consider the comparisons above under a new context: we limit the amount of compute, not the number of samples. We contend that when training in simulation compute efficiency should be considered an equal counterpart. In Apx. B we detail improvements we make to Habitat’s compute utilization.

Samples Used. To enable clean comparisons with future work, we convert compute back into a number of sam-

#	Sensors	Norm Adv.	HyperParams	SimpleCNN				ResNet18			
				Gibson		Matterport3D		Gibson		Matterport3D	
				Success \uparrow	SPL \uparrow	Success \uparrow	SPL \uparrow	Success \uparrow	SPL \uparrow	Success \uparrow	SPL \uparrow
1	RGB	✓	Set 1	11.3 \pm 5.25	08.6 \pm 3.88	01.0 \pm 0.18	00.8 \pm 0.15	59.0 \pm 3.46	41.8 \pm 4.50	24.8 \pm 1.35	20.3 \pm 1.43
2		-	Set 1	34.0 \pm 12.15	25.2 \pm 8.58	01.1 \pm 0.24	01.0 \pm 0.21	50.9 \pm 4.14	37.6 \pm 2.37	15.3 \pm 1.75	13.1 \pm 1.56
3		✓	Set 2	00.0 \pm 0.00	00.0 \pm 0.00	00.0 \pm 0.00	00.0 \pm 0.00	63.1 \pm 4.48	49.8 \pm 3.79	29.4 \pm 3.73	24.3 \pm 1.91
4		-	Set 2	46.2 \pm 11.66	32.8 \pm 9.00	02.3 \pm 0.86	01.9 \pm 0.66	68.3 \pm 2.95	51.5 \pm 1.63	22.3 \pm 1.49	19.4 \pm 0.65
5	RGB-D	✓	Set 1	68.2 \pm 1.97	51.2 \pm 3.86	21.1 \pm 4.45	15.7 \pm 2.31	73.4 \pm 1.53	59.8 \pm 1.31	52.1 \pm 1.56	38.3 \pm 0.67
6		-	Set 1	64.0 \pm 5.42	49.1 \pm 3.52	21.0 \pm 7.72	16.0 \pm 5.50	72.9 \pm 3.04	56.6 \pm 0.81	48.4 \pm 2.83	40.2 \pm 1.26
7		✓	Set 2	75.8 \pm 3.83	65.0 \pm 4.03	44.6 \pm 25.38	34.4 \pm 19.47	81.2 \pm 1.67	68.8 \pm 1.51	58.1 \pm 5.24	47.0 \pm 3.38
8		-	Set 2	78.8 \pm 1.47	66.2 \pm 1.42	57.7 \pm 2.43	42.1 \pm 1.61	80.8 \pm 2.47	68.0 \pm 1.60	61.2 \pm 2.27	50.4 \pm 1.99
9	Depth	✓	Set 1	77.5 \pm 0.68	64.5 \pm 2.49	49.1 \pm 6.28	38.7 \pm 2.80	78.0 \pm 3.80	64.7 \pm 4.37	55.1 \pm 1.00	42.9 \pm 1.25
10		-	Set 1	75.0 \pm 1.96	62.4 \pm 2.08	46.7 \pm 5.18	37.6 \pm 3.54	74.2 \pm 2.69	60.5 \pm 1.09	54.8 \pm 2.69	44.9 \pm 2.26
11		✓	Set 2	81.4 \pm 1.61	71.7 \pm 2.20	67.1 \pm 4.08	52.7 \pm 3.10	80.8 \pm 3.17	68.1 \pm 4.41	62.2 \pm 2.34	50.0 \pm 1.90
12		-	Set 2	87.1 \pm 1.44	74.2 \pm 0.67	67.1 \pm 2.83	53.5 \pm 2.65	83.0 \pm 1.23	71.4 \pm 1.63	63.2 \pm 0.63	52.4 \pm 0.95

Table 2: **Results on PointGoalNav at 1 GPU-day.** Performance reported on the Gibson and Matterport3D validation sets. Under a fixed compute regime, we find that ResNet18 improves performance for RGB and RGB-D agents while the increased number of samples achievable with SimpleCNN is beneficial for Depth agents. Mean and 95% CI from 5 runs.

Visual Encoder	Hyper parameters	Throughput (Samples per Second)	Total (Millions)	Factor
ResNet18	1	100	8.0	1.00
ResNet18	2	120	10.0	1.25
SimpleCNN	1	170	14.0	1.75
SimpleCNN	2	200	16.0	2.00

Figure 4: **Training speed** of the various settings considered this work. All numbers reported for RGB agents on the Matterport3D [5] dataset. Times measure on a single 2080Ti GPU.

#	Sensors	Depth	Gibson	
			Success \uparrow	SPL \uparrow
1	RGB	1	69.5 \pm 1.76	53.3 \pm 1.48
2		2	68.1 \pm 2.29	50.2 \pm 1.33
3	RGB-D	1	78.8 \pm 0.67	68.3 \pm 0.37
4		2	79.3 \pm 0.72	67.8 \pm 1.14

Table 3: **Comparison of RNN Depth.** We find that a second RNN layer does not help RGB-D agents and may harm RGB agents. Mean and 95% CI from 5 runs.

ples, but encourage researches to stick the spirit of 1 GPU-day and adjust the number of samples if their method considerably changes the number of samples that can be obtained under this compute budget. In Tab. 4 we list the training throughput (in number of samples per second) for the agent configurations (both architecture and hyper-parameters) studied in this work. We will compare agents trained for a different number of samples but all under a similar amount of compute.

6. Results on a Compute Budget

We compare and contrast the trends found when training for a fixed number of samples in Sec. 4 with a fixed compute budget of 1 GPU-day. We examine the same variants as in Sec. 4 and use the same method to describe results. Tab. 2 show these results. We describe the trends below:

Hyper-parameter set 2 continues to outperform hyper-parameter set 1 for all variations. This effect is now compounded by the $\sim 25\%$ more samples that can be collected under hyper-parameter set 2. Under a fixed number of samples (10M for ResNet18 and 16M for SimpleCNN), the average improvement when switching from hyper-parameter set 1 to 2 is 8.0 ± 2.75 SPL, which under a fixed compute budget (1 GPU-day), the average improvement is 9.3 ± 2.75 SPL.

Normalized advantage is inconsistent, sometimes harming performance ($-3.3/-2.4$ SPL, Tab. 2, row 11 vs. 12, ResNet18) and sometimes improving performance ($-1.7/+4.9$ SPL, Tab. 2, row 3 vs. 4, ResNet18). We hypothesize that early in training, normalized advantage increases the weight of the policy loss, causing the agent to more optimize for initial performance at the cost of final performance.

RGB favors ResNet18, Depth-only favors SimpleCNN. The largest difference due to the fixed compute regime is ResNet18 vs. SimpleCNN. Under the fixed sample regime, ResNet18 is a better choice regardless of visual input. Under a fixed compute regime however, the significant increase in the number of samples that can be collected with SimpleCNN allows it to outperform ResNet18 for Depth-only agents in all cases except Matterport3D with hyper-parameter set 1. This is perhaps why researchers may have been using SimpleCNN [1, 28, 25, 29] – under a given compute budget, it does perform better when the visual representation is already close to correct for the task.

NumSim	RolloutLength									
	32		48		64		96		128	
	Success \uparrow	SPL \uparrow								
2	08.4 \pm 5.56	07.3 \pm 4.78	12.2 \pm 3.22	10.2 \pm 2.52	18.2 \pm 2.17	16.3 \pm 1.97	23.0 \pm 4.38	20.6 \pm 4.15	28.4 \pm 1.89	24.3 \pm 1.42
4	21.9 \pm 1.40	19.3 \pm 1.04	22.3 \pm 1.49	19.9 \pm 1.43	26.1 \pm 3.60	23.4 \pm 2.96	29.6 \pm 1.24	25.5 \pm 1.09	34.4 \pm 4.02	28.5 \pm 4.27
6	23.9 \pm 6.11	21.4 \pm 5.34	26.2 \pm 1.51	22.9 \pm 1.16	32.1 \pm 1.24	27.5 \pm 1.16	33.5 \pm 1.80	27.9 \pm 0.94	38.5 \pm 2.29	30.6 \pm 1.37

Table 4: **Hyper-parameter analysis.** Results of hyperparameter analysis at 40 million frames. We find that, in general, performance improves as the number of steps collected per rollout (NumSim \times RolloutLength) increases and there isn’t a significant trade-off between reducing either to reduce GPU memory. Mean and 95% CI from 5 runs.

For RGB agents, ResNet18 continues to be a better choice – so much so that a ResNet18 RGB agent trained with hyper-parameter set 1 out-performs a SimpleCNN RGB agent trained under hyper-parameter set 2, +3.8/+11.2 SPL (Tab. 2, row 4 vs. 2), despite the 2x sample difference between the two. Interestingly, for RGB-D agents, ResNet18 continues to outperform SimpleCNN, hinting that the primary benefit ResNet18 brings for RGB-D agents is the ability to more effectively learn to ignore the RGB component.

Does RNN Depth Matter? In the context of a compute budget, we examine whether RNN depth matters. Interestingly, RNN depth does not have a measure impact on the number of samples that can be obtained and thereby provides ‘free’ additional network capacity. We examine if this improves performance for RGB and RGB-D agents on the Gibson dataset using ResNet18 and hyper-parameter set 2 (our most best setting for these agents). Tab. 3 shows these results. Interestingly, we find that the extra layer makes no difference for RGB-D and likely harms performance for RGB.

7. Analysis

In this section we provide additional analysis on two trends highlighted in our results, the impact of batch size and the negative impact of normalized advantage.

7.1. Batch Size

One surprising trend from our analysis is that of hyper-parameter set 2 improves both sample efficiency *and* compute efficiency. The improvements in compute efficiency are intuitive, they are due to using a large mini-batch size during learning (which leads to better GPU utilization and less over-all gradient updates). However, the improvements to sample efficiency are less intuitive. To investigate, we systematically analyze different mini-batch sizes⁴.

The number of steps of experience per mini-batch is defined as follows: Let NumSim be the number of parallel simulators, RolloutLength be the number of steps of experience collected from each per rollout, and NumMiniBatch be the number of PPO mini-batches, then the number

⁴Note that this experiment was performed after we had the results presented thus far and was not used to inform the choices of the hyper-parameter sets.

of steps of experience per mini-batch is $\frac{\text{NumSim}}{\text{NumMiniBatch}} \times \text{RolloutLength}$. We fix NumMiniBatch=2 and examine all combinations of NumSim $\in \{2, 4, 6\}$ and RolloutLength $\in \{32, 48, 64, 96, 128\}$. We examine their effect on RGB ResNet18 agents without normalized advantage on the Matterport3D dataset as it is the most taxing sensor/dataset combination (lowest performance). To examine sample efficiency, we train for 40 million steps of experience. We note that the settings with shorter RolloutLength or lower NumSim are less compute efficient⁵.

We find that, overall, a larger batch size is more sample efficient (see the monotonic improvement in performance in Tab. 4). In the context of PointGoalNav with 1-GPU, *a larger batch size is more sample efficient* despite reducing the total number of parameter updates and increasing the amount of experience gathered between updates. This is likely due to reducing the variance [48] and increasing the number of positive examples in the mini-batch.

We find that NumSim=2 tends to under perform, for instance NumSim=2 RolloutLength=64 collects the same amount of experience per update as NumSim=4 RolloutLength=32 but results in -6 Success, -5 SPL, Tab. 4. We hypothesis that NumSim=2 underperforms as, with NumMiniBatch=2, each batch has experience from the same environment, leading to highly correlated data within a batch. For the other values of NumSim, there isn’t any particular trade-off between reducing NumSim or RolloutLength.

7.2. Normalized Advantage

Despite its near ubiquity in advantage actor-critic methods (like PPO), we find normalized advantage to be harmful. To investigate this trend, we tested two possible hypothesis for why normalized advantage is harmful:

- 1) Division by a small standard deviation. Early in training, advantages can be quite small and division by a small standard deviation would cause gradient spikes.
- 2) Variance in the estimate of normalization parameters later in training. Later in training, advantages become larger in size (and thus larger variance), however, the normalization parameters are estimated per mini-batch

⁵The NumSim=2 RolloutLength=32 setting took 2 weeks!

#	Sensors	Policy	Gibson	
			SPL@Compute \uparrow	SPL@Sample \uparrow
1	RGB	SimpleCNN	40.1 \pm 3.31	61.8 \pm 0.96
2		ResNet18	52.6 \pm 2.08	66.4 \pm 1.28

Table 5: **Second Normalized Advantage Method.** Results of a second variant of normalized advantage with hyperparameter set 2. While this method is not harmful performance, it still introduces instability.

and poorly estimated normalization parameters may lead to divergence.

We test both these possibilities by 1) clipping the minimum value for the estimated standard deviation to 1, *i.e.* $\sigma = \max(\sigma, 1)$ and 2) utilizing an exponential moving average of mean and variance. This procedure is the same as that used in Mnih *et al.* [49].

We examine this for RGB agents on Gibson using Hyperparameter Set 2 for both SimpleCNN and ResNet18 agents as it was harmful to the former and non-influential to the latter, results in Tab. 5. For ResNet18, this variant is not statistically different from per mini-batch or no normalization in either regime (52.6/66.4 SPL vs. 49.8/68.0 SPL vs. 51.5/68.4 SPL – Tab. 5 row 2 vs. Tab. 1 row 3/4 vs. Tab. 2 row 3). For SimpleCNN, this variant outperforms per mini-batch normalization in both regimes (40.1/61.8 SPL vs. 0.0/11.2). It outperforms no normalization in the compute-limited regime while both are on-par in the sample limited regime (32.8/63.2). This indicates that a small variance likely explains the initial harm in performance. However the instability later in training remains, indicating that neither effect fully explain this phenomena. This opens an interesting avenue for future work to develop an advantage normalization scheme that improves initial performance without causing instability.

8. Discussion

In this work we have proposed that when training in simulation compute efficiency should be an equal counterpart to sample efficiency. We argue that when training in simulation, the cost of a sample is due to the compute needed to generate it and learn from it, not something intrinsic to the sample itself. When training in reality however, the cost to obtain a sample (monetary and time cost of the both the robot and its operator) dramatically outweighs the computation cost of learning from the sample, thus the focus has duly been put on sample efficiency (or when training in simulation as a direct stand-in for reality). However, training in simulation, be it for evaluation in solely simulation, pre-training before fine-tuning in reality, or for zero-shot sim2real, is becoming increasingly popular and we argue that compute efficiency should be considered equally important in this context.

We note that reproducibility of results under a compute budget is challenging – different simulators run at different speeds, existing simulators, GPU hardware, CUDA, and cuDNN get faster, *etc.* Given these challenges, comparisons under precisely the same compute budget is not feasible. Instead, we encourage researchers to examine the the compute efficiency of their proposed method and compare against prior work under *similar* compute budgets.

We present experiments and analysis of how ostensibly minor changes influence both the sample efficiency and compute efficiency of embodied agents. Boiling them down, we draw the following primary findings:

Use a deeper CNN, *e.g.* ResNet18. Due to its long use in reinforcement learning for video games (*i.e.* Atari), the CNN from [46] has also been adopted for visual navigation (it is the default in both Habitat [1] and AllenAct [29]). Our results show that this CNN is outperformed by ResNet18 – not just in terms of accuracy (which is expected) but also in compute efficiency and sample efficiency, which is a surprising and counterintuitive finding – priori we might expect larger models to be *less* efficient, not more. This also goes against the trend in continuous control where larger CNNs harm performance without augmentation [38]. We expect this trend will hold for tasks that rely even more on visual recognition, like ObjectGoal navigation [19], question answering [13], object rearrangement [50], *etc.*

Use large and diverse mini-batches. The effect of batch size for compute efficiency is perhaps expected, however, it is quite surprising for sample efficiency. In the setting of learning in realistic simulators, the batch size is often constrained by GPU memory, limiting the feasible range one would search. Our results show that even a seemingly large batch size of 3×64 is not large enough. Second, we show that NumSim=2 consistently underperforms. While this is a natural choice to reduce the GPU memory footprint of simulation, our results show that this is a suboptimal choice and other techniques need to be employed to fit within the GPU memory limit. We expect these overall trends, larger batch sizes improve sample efficiency, and NumSim=2 underperforms, to hold true on other tasks as these control the gradient variance and diversity in the mini batch, which is not task specific. Further, there is evidence that harder tasks require even larger batch sizes [51].

Do not use normalized advantage . Normalized advantage is a nearly ubiquitous trick in advantage actor critic methods that have been tuned for single environment reinforcement learning. We show that this widely prevalent trick can be harmful for embodied navigation while providing little-to-no benefit when it isn't.

We encourage researchers to compare against these agents trained with these tips and tricks and use them (where applicable) to ensure that advances build upon known best practices instead of rectifying for their absence.

9. Acknowledgements

EW is supported in part by an ARCS fellowship. The Georgia Tech effort was supported in part by NSF, AFRL, DARPA, ONR YIPs, ARO PECASE. The views and conclusions contained herein are those of the authors and should not be interpreted as necessarily representing the official policies or endorsements, either expressed or implied, of the U.S. Government, or any sponsor.

References

- [1] Manolis Savva, Abhishek Kadian, Oleksandr Maksymets, Yili Zhao, Erik Wijmans, Bhavana Jain, Julian Straub, Jia Liu, Vladlen Koltun, Jitendra Malik, Devi Parikh, and Dhruv Batra. Habitat: A Platform for Embodied AI Research. In *Proceedings of IEEE International Conference on Computer Vision (ICCV)*, 2019.
- [2] Fei Xia, William B Shen, Chengshu Li, Priya Kasimbeg, Micael Edmond Tchampi, Alexander Toshev, Roberto Martín-Martín, and Silvio Savarese. Interactive gibbon benchmark: A benchmark for interactive navigation in cluttered environments. *IEEE Robotics and Automation Letters*, 5(2):713–720, 2020.
- [3] Manolis Savva, Angel X. Chang, Alexey Dosovitskiy, Thomas Funkhouser, and Vladlen Koltun. MINOS: Multimodal indoor simulator for navigation in complex environments. *arXiv:1712.03931*, 2017.
- [4] Julian Straub, Thomas Whelan, Lingni Ma, Yufan Chen, Erik Wijmans, Simon Green, Jakob J. Engel, Raul Mur-Artal, Carl Ren, Shobhit Verma, Anton Clarkson, Mingfei Yan, Brian Budge, Yajie Yan, Xiaqing Pan, June Yon, Yuyang Zou, Kimberly Leon, Nigel Carter, Jesus Briales, Tyler Gillingham, Elias Mueggler, Luis Pesqueira, Manolis Savva, Dhruv Batra, Hauke M. Strasdat, Renzo De Nardi, Michael Goesele, Steven Lovegrove, and Richard Newcombe. The Replica dataset: A digital replica of indoor spaces. *arXiv preprint arXiv:1906.05797*, 2019.
- [5] Angel Chang, Angela Dai, Thomas Funkhouser, Maciej Halber, Matthias Niessner, Manolis Savva, Shuran Song, Andy Zeng, and Yinda Zhang. Matterport3d: Learning from rgb-d data in indoor environments. *International Conference on 3D Vision (3DV)*, 2017. MatterPort3D dataset license available at: <http://kaldir.vc.in.tum.de/matterport/MP-TOS.pdf>.
- [6] Fei Xia, Amir R Zamir, Zhiyang He, Alexander Sax, Jitendra Malik, and Silvio Savarese. Gibson env: Real-world perception for embodied agents. In *Proceedings of IEEE Conference on Computer Vision and Pattern Recognition (CVPR)*, 2018. Gibson dataset license agreement available at https://storage.googleapis.com/gibson_material/Agreement%20GDS%2006-04-18.pdf.
- [7] David Silver, Julian Schrittwieser, Karen Simonyan, Ioannis Antonoglou, Aja Huang, Arthur Guez, Thomas Hubert, Lucas Baker, Matthew Lai, Adrian Bolton, et al. Mastering the game of go without human knowledge. *Nature*, 550(7676):354, 2017.
- [8] Yuandong Tian, Jerry Ma, Qucheng Gong, Shubho Sengupta, Zhuoyuan Chen, James Pinkerton, and C Lawrence Zitnick. Elf opengo: An analysis and open reimplementation of alphazero. *arXiv preprint arXiv:1902.04522*, 2019.
- [9] OpenAI. Openai five. <https://blog.openai.com/openai-five/>, 2018.
- [10] Peter Anderson, Angel Chang, Devendra Singh Chaplot, Alexey Dosovitskiy, Saurabh Gupta, Vladlen Koltun, Jana Kosecka, Jitendra Malik, Roozbeh Mottaghi, Manolis Savva, et al. On Evaluation of Embodied Navigation Agents. *arXiv preprint arXiv:1807.06757*, 2018.
- [11] Peter Anderson, Qi Wu, Damien Teney, Jake Bruce, Mark Johnson, Niko Sünderhauf, Ian Reid, Stephen Gould, and Anton van den Hengel. Vision-and-language navigation: Interpreting visually-grounded navigation instructions in real environments. In *Proceedings of IEEE Conference on Computer Vision and Pattern Recognition (CVPR)*, 2018.
- [12] Mohit Shridhar, Jesse Thomason, Daniel Gordon, Yonatan Bisk, Winson Han, Roozbeh Mottaghi, Luke Zettlemoyer, and Dieter Fox. ALFRED: A Benchmark for Interpreting Grounded Instructions for Everyday Tasks. In *Proceedings of IEEE Conference on Computer Vision and Pattern Recognition (CVPR)*, 2020.
- [13] Abhishek Das, Samyak Datta, Georgia Gkioxari, Stefan Lee, Devi Parikh, and Dhruv Batra. Embodied Question Answering. In *Proceedings of IEEE Conference on Computer Vision and Pattern Recognition (CVPR)*, 2018.
- [14] Daniel Gordon, Aniruddha Kembhavi, Mohammad Rastegari, Joseph Redmon, Dieter Fox, and Ali Farhadi. Iqa: Visual question answering in interactive environments. In *Proceedings of IEEE Conference on Computer Vision and Pattern Recognition (CVPR)*, pages 4089–4098, 2018.
- [15] Erik Wijmans, Samyak Datta, Oleksandr Maksymets, Abhishek Das, Georgia Gkioxari, Stefan Lee, Irfan Essa, Devi Parikh, and Dhruv Batra. Embodied question answering in photorealistic environments with point cloud perception. In *Proceedings of IEEE Conference on Computer Vision and Pattern Recognition (CVPR)*, pages 6659–6668, 2019.
- [16] Erik Wijmans, Abhishek Kadian, Ari Morcos, Stefan Lee, Irfan Essa, Devi Parikh, Manolis Savva, and Dhruv Batra. DD-PPO: Learning near-perfect pointgoal navigators from 2.5 billion frames. In *Proceedings of the International Conference on Learning Representations (ICLR)*, 2020.
- [17] Santhosh K Ramakrishnan, Ziad Al-Halah, and Kristen Grauman. Occupancy anticipation for efficient exploration and navigation. In *Proceedings of European Conference on Computer Vision (ECCV)*, pages 400–418. Springer, 2020.
- [18] Samyak Datta, Oleksandr Maksymets, Judy Hoffman, Stefan Lee, Dhruv Batra, and Devi Parikh. Integrating egocentric localization for more realistic point-goal navigation agents. *Proceedings of the Conference on Robot Learning (CoRL)*, 2020.
- [19] Dhruv Batra, Aaron Gokaslan, Aniruddha Kembhavi, Oleksandr Maksymets, Roozbeh Mottaghi, Manolis Savva, Alexander Toshev, and Erik Wijmans. Objectnav revisited: On evaluation of embodied agents navigating to objects. *arXiv preprint arXiv:2006.13171*, 2020.

- [20] Devendra Singh Chaplot, Dhiraj Prakashchand Gandhi, Abhinav Gupta, and Russ R Salakhutdinov. Object goal navigation using goal-oriented semantic exploration. *Advances in Neural Information Processing Systems (NIPS)*, 33, 2020.
- [21] Medhini Narasimhan, Erik Wijmans, Xinlei Chen, Trevor Darrell, Dhruv Batra, Devi Parikh, and Amanpreet Singh. Seeing the un-scene: Learning amodal semantic maps for room navigation. *arXiv preprint arXiv:2007.09841*, 2020.
- [22] Abhishek Kadian, Joanne Truong, Aaron Gokaslan, Alexander Clegg, Erik Wijmans, Stefan Lee, Manolis Savva, Sonia Chernova, and Dhruv Batra. Are we making real progress in simulated environments? measuring the sim2real gap in embodied visual navigation. *IEEE Robotics and Automation Letters (RA-L)*, 2019.
- [23] Joel Ye, Dhruv Batra, Erik Wijmans, and Abhishek Das. Auxiliary tasks speed up learning pointgoal navigation. *Proceedings of the Conference on Robot Learning (CoRL)*, 2020.
- [24] Devendra Singh Chaplot, Dhiraj Gandhi, Saurabh Gupta, Abhinav Gupta, and Ruslan Salakhutdinov. Learning to explore using active neural slam. *Proceedings of the International Conference on Learning Representations (ICLR)*, 2020.
- [25] Alexander Sax, Jeffrey O Zhang, Bradley Emi, Amir Zamir, Silvio Savarese, Leonidas Guibas, and Jitendra Malik. Learning to navigate using mid-level visual priors. *Proceedings of the Conference on Robot Learning (CoRL)*, 2019.
- [26] Matt Deitke, Winson Han, Alvaro Herrasti, Aniruddha Kembhavi, Eric Kolve, Roozbeh Mottaghi, Jordi Salvador, Dustin Schwenk, Eli VanderBilt, Matthew Wallingford, et al. Robothon: An open simulation-to-real embodied ai platform. In *Proceedings of IEEE Conference on Computer Vision and Pattern Recognition (CVPR)*, pages 3164–3174, 2020.
- [27] Eric Kolve, Roozbeh Mottaghi, Winson Han, Eli VanderBilt, Luca Weihs, Alvaro Herrasti, Daniel Gordon, Yuke Zhu, Abhinav Gupta, and Ali Farhadi. AI2-THOR: An Interactive 3D Environment for Visual AI. *arXiv*, 2017.
- [28] Daniel Gordon, Abhishek Kadian, Devi Parikh, Judy Hoffman, and Dhruv Batra. Splitnet: Sim2sim and task2task transfer for embodied visual navigation. In *Proceedings of IEEE International Conference on Computer Vision (ICCV)*, 2019.
- [29] Luca Weihs, Jordi Salvador, Klemen Kotar, Unnat Jain, Kuo-Hao Zeng, Roozbeh Mottaghi, and Aniruddha Kembhavi. Allenact: A framework for embodied ai research. *arXiv preprint arXiv:2008.12760*, 2020.
- [30] Kaiming He, Xiangyu Zhang, Shaoqing Ren, and Jian Sun. Deep residual learning for image recognition. In *Proceedings of IEEE Conference on Computer Vision and Pattern Recognition (CVPR)*, 2016.
- [31] Logan Engstrom, Andrew Ilyas, Shibani Santurkar, Dimitris Tsipras, Firdaus Janoos, Larry Rudolph, and Aleksander Madry. Implementation matters in deep rl: A case study on ppo and trpo. In *Proceedings of the International Conference on Learning Representations (ICLR)*, 2020.
- [32] John Schulman, Filip Wolski, Prafulla Dhariwal, Alec Radford, and Oleg Klimov. Proximal policy optimization algorithms. *CoRR*, abs/1707.06347, 2017.
- [33] Tuomas Haarnoja, Aurick Zhou, Pieter Abbeel, and Sergey Levine. Soft actor-critic: Off-policy maximum entropy deep reinforcement learning with a stochastic actor. *Proceedings of the International Conference on Machine Learning (ICML)*, 2018.
- [34] Zhaohan Daniel Guo, Mohammad Gheshlaghi Azar, Bilal Piot, Bernardo A Pires, and Rémi Munos. Neural predictive belief representations. *arXiv preprint arXiv:1811.06407*, 2018.
- [35] Daniel Guo, Bernardo Avila Pires, Bilal Piot, Jean-bastien Grill, Florent Altché, Rémi Munos, and Mohammad Gheshlaghi Azar. Bootstrap latent-predictive representations for multitask reinforcement learning. *Proceedings of the International Conference on Machine Learning (ICML)*, 2020.
- [36] Aravind Srinivas, Michael Laskin, and Pieter Abbeel. Curl: Contrastive unsupervised representations for reinforcement learning. *Proceedings of the International Conference on Machine Learning (ICML)*, 2020.
- [37] Deepak Pathak, Dhiraj Gandhi, and Abhinav Gupta. Self-supervised exploration via disagreement. *Proceedings of the International Conference on Machine Learning (ICML)*, 2019.
- [38] Ilya Kostrikov, Denis Yarats, and Rob Fergus. Image augmentation is all you need: Regularizing deep reinforcement learning from pixels. *arXiv preprint arXiv:2004.13649*, 2020.
- [39] Michael Laskin, Kimin Lee, Adam Stooke, Lerrel Pinto, Pieter Abbeel, and Aravind Srinivas. Reinforcement learning with augmented data. *arXiv:2004.14990*, 2020.
- [40] Aleksei Petrenko, Zhehui Huang, Tushar Kumar, Gaurav Sukhatme, and Vladlen Koltun. Sample factory: Egocentric 3d control from pixels at 100000 fps with asynchronous reinforcement learning. *Proceedings of the International Conference on Machine Learning (ICML)*, 2020.
- [41] Lasse Espeholt, Hubert Soyer, Rémi Munos, Karen Simonyan, Volodymyr Mnih, Tom Ward, Yotam Doron, Vlad Firoiu, Tim Harley, Iain Dunning, et al. Impala: Scalable distributed deep-rl with importance weighted actor-learner architectures. *Proceedings of the International Conference on Machine Learning (ICML)*, 2018.
- [42] Mahmoud Assran, Joshua Romoff, Nicolas Ballas, Joelle Pineau, and Michael Rabbat. Gossip-based actor-learner architectures for deep reinforcement learning. In *Advances in Neural Information Processing Systems (NIPS)*, pages 13320–13330, 2019.
- [43] Marcin Andrychowicz, Anton Raichuk, Piotr Stańczyk, Manu Orsini, Sertan Girgin, Raphael Marinier, Léonard Hussenot, Matthieu Geist, Olivier Pietquin, Marcin Michalski, et al. What matters in on-policy reinforcement learning? a large-scale empirical study. *arXiv preprint arXiv:2006.05990*, 2020.
- [44] Yuxin Wu and Kaiming He. Group normalization. In *Proceedings of European Conference on Computer Vision (ECCV)*, 2018.
- [45] John Schulman, Philipp Moritz, Sergey Levine, Michael Jordan, and Pieter Abbeel. High-dimensional continuous control using generalized advantage estimation. *Proceedings of*

the International Conference on Learning Representations (ICLR), 2016.

- [46] Volodymyr Mnih, Koray Kavukcuoglu, David Silver, Alex Graves, Ioannis Antonoglou, Daan Wierstra, and Martin Riedmiller. Playing atari with deep reinforcement learning. *arXiv preprint arXiv:1312.5602*, 2013.
- [47] Sergey Ioffe and Christian Szegedy. Batch normalization: Accelerating deep network training by reducing internal covariate shift. *arXiv preprint arXiv:1502.03167*, 2015.
- [48] Samuel L Smith, Pieter-Jan Kindermans, Chris Ying, and Quoc V Le. Don't decay the learning rate, increase the batch size. *Proceedings of the International Conference on Learning Representations (ICLR)*, 2018.
- [49] Andriy Mnih and Karol Gregor. Neural variational inference and learning in belief networks. *Proceedings of the International Conference on Machine Learning (ICML)*, 2014.
- [50] Dhruv Batra, Angel X Chang, Sonia Chernova, Andrew J Davison, Jia Deng, Vladlen Koltun, Sergey Levine, Jitendra Malik, Igor Mordatch, Roozbeh Mottaghi, Manolis Savva, and Hao Su. Rearrangement: A challenge for embodied ai. *arXiv preprint arXiv:2011.01975*, 2020.
- [51] Sam McCandlish, Jared Kaplan, Dario Amodei, and OpenAI Dota Team. An empirical model of large-batch training. *arXiv preprint arXiv:1812.06162*, 2018.
- [52] Adam Stooke and Pieter Abbeel. rlpyt: A research code base for deep reinforcement learning in pytorch. *arXiv preprint arXiv:1909.01500*, 2019.
- [53] Diederik P Kingma and Jimmy Ba. Adam: A method for stochastic optimization. *Proceedings of the International Conference on Learning Representations (ICLR)*, 2015.

A. Additional Break Down

We provide additional break downs of our main results on sample efficiency at different sample budgets.

B. Improvements to compute utilization.

Since our goal is maximize our performance given a fixed compute budget, we first make improvements to the habitat-baselines code-base to improve training throughput for *all* models studied.⁶ The largest improvement is due to utilizing a Double Buffered [40]/Alternating-GPU [52] sampler that allows for 20% more samples to be collected under a given compute budget. While collecting experience in the rollout, these sampling methods break the environments running in parallel into two groups. Half the environments will simulate the result of taking the next action while the policy is executed to select the next action for the other half. This allows network inference and simulation to be interleaved, leading to better usage of the PCIe bus, the fixed functions on the GPU that are dedicated to rendering, and a reduction in synchronization overhead. We make additional minor improvements that result in another 10%-15% training speed.

⁶We will make code publicly available.

#	Sensors	Norm Adv.	HyperParams	SimpleCNN				ResNet18			
				Gibson		Matterport3D		Gibson		Matterport3D	
				Success \uparrow	SPL \uparrow	Success \uparrow	SPL \uparrow	Success \uparrow	SPL \uparrow	Success \uparrow	SPL \uparrow
1	RGB	✓	Set 1	07.4 \pm 0.93	05.9 \pm 0.82	01.0 \pm 0.18	00.8 \pm 0.15	57.6 \pm 3.81	42.3 \pm 4.39	24.9 \pm 1.34	20.5 \pm 1.40
2		-	Set 1	11.1 \pm 2.39	08.7 \pm 1.71	01.1 \pm 0.24	00.9 \pm 0.22	57.1 \pm 1.69	41.4 \pm 0.94	19.0 \pm 5.31	15.6 \pm 3.39
3		✓	Set 2	00.0 \pm 0.00	00.0 \pm 0.00	00.0 \pm 0.00	00.0 \pm 0.00	63.1 \pm 4.48	49.8 \pm 3.79	29.4 \pm 3.73	24.3 \pm 1.91
4		-	Set 2	15.7 \pm 2.07	11.6 \pm 1.01	01.7 \pm 0.88	01.4 \pm 0.62	68.3 \pm 2.95	51.5 \pm 1.63	22.3 \pm 1.49	19.4 \pm 0.65
5	RGB-D	✓	Set 1	60.4 \pm 9.60	46.1 \pm 6.61	07.6 \pm 2.41	06.1 \pm 2.00	74.3 \pm 1.10	61.1 \pm 0.82	51.9 \pm 1.58	39.5 \pm 0.97
6		-	Set 1	48.6 \pm 11.29	36.9 \pm 9.19	07.1 \pm 1.05	05.8 \pm 0.90	72.1 \pm 1.99	57.4 \pm 1.64	49.0 \pm 2.67	40.7 \pm 1.04
7		✓	Set 2	69.1 \pm 4.52	57.6 \pm 4.35	44.5 \pm 19.57	34.6 \pm 15.24	81.2 \pm 1.67	68.8 \pm 1.51	58.1 \pm 5.24	47.0 \pm 3.38
8		-	Set 2	76.8 \pm 1.83	61.4 \pm 0.87	52.5 \pm 4.43	37.5 \pm 3.03	80.8 \pm 2.47	68.0 \pm 1.60	61.2 \pm 2.27	50.4 \pm 1.99
9	Depth	✓	Set 1	70.3 \pm 2.46	57.3 \pm 2.06	41.1 \pm 7.52	32.8 \pm 5.25	80.4 \pm 3.20	67.7 \pm 2.15	56.4 \pm 0.97	43.2 \pm 1.28
10		-	Set 1	71.5 \pm 1.51	57.1 \pm 1.02	33.5 \pm 5.24	26.7 \pm 3.16	76.0 \pm 1.91	62.2 \pm 1.28	55.1 \pm 2.26	45.3 \pm 1.72
11		✓	Set 2	77.7 \pm 2.03	67.1 \pm 2.19	63.2 \pm 4.25	49.8 \pm 2.99	80.8 \pm 3.17	68.1 \pm 4.41	62.2 \pm 2.34	50.0 \pm 1.90
12		-	Set 2	82.4 \pm 2.93	70.1 \pm 0.60	60.1 \pm 3.69	44.2 \pm 2.12	83.0 \pm 1.23	71.4 \pm 1.63	63.2 \pm 0.63	52.4 \pm 0.95

Table A1: Results on PointGoalNav at 10 million. Same as Tab. 1 but at 10 million steps.

#	Sensors	Norm Adv.	HyperParams	SimpleCNN				ResNet18			
				Gibson		Matterport3D		Gibson		Matterport3D	
				Success \uparrow	SPL \uparrow	Success \uparrow	SPL \uparrow	Success \uparrow	SPL \uparrow	Success \uparrow	SPL \uparrow
1	RGB	✓	Set 1	31.7 \pm 10.29	23.3 \pm 7.46	01.7 \pm 0.98	01.4 \pm 0.75	63.1 \pm 3.31	47.0 \pm 1.85	32.3 \pm 2.95	25.7 \pm 1.27
2		-	Set 1	47.4 \pm 3.26	33.0 \pm 2.71	01.4 \pm 0.18	01.2 \pm 0.14	65.1 \pm 2.43	50.0 \pm 1.27	25.2 \pm 2.63	20.4 \pm 1.47
3		✓	Set 2	00.0 \pm 0.00	00.0 \pm 0.00	00.0 \pm 0.00	00.0 \pm 0.00	73.3 \pm 3.69	58.4 \pm 2.67	36.2 \pm 2.12	30.0 \pm 1.30
4		-	Set 2	52.9 \pm 5.24	37.2 \pm 5.13	03.3 \pm 1.20	02.8 \pm 0.98	70.2 \pm 1.28	56.0 \pm 0.97	29.4 \pm 3.56	25.1 \pm 2.35
5	RGB-D	✓	Set 1	69.5 \pm 1.30	56.2 \pm 2.03	37.2 \pm 8.69	28.2 \pm 5.87	80.5 \pm 1.58	70.4 \pm 1.66	61.3 \pm 2.39	48.1 \pm 2.60
6		-	Set 1	70.0 \pm 2.65	55.0 \pm 2.20	27.7 \pm 7.42	21.7 \pm 5.39	78.9 \pm 2.79	67.0 \pm 1.83	63.1 \pm 2.83	50.1 \pm 1.55
7		✓	Set 2	78.5 \pm 3.71	66.9 \pm 3.23	45.6 \pm 25.96	34.4 \pm 19.49	85.5 \pm 0.91	75.2 \pm 0.84	65.5 \pm 2.60	54.0 \pm 0.90
8		-	Set 2	80.4 \pm 0.91	67.2 \pm 1.56	59.2 \pm 3.33	45.0 \pm 2.15	85.4 \pm 1.20	73.9 \pm 1.00	65.7 \pm 2.02	55.1 \pm 1.17
9	Depth	✓	Set 1	76.7 \pm 2.18	66.5 \pm 1.78	55.3 \pm 3.53	42.4 \pm 2.53	83.2 \pm 1.68	74.0 \pm 1.26	60.7 \pm 1.24	48.3 \pm 1.54
10		-	Set 1	77.0 \pm 2.54	65.2 \pm 1.92	59.1 \pm 5.11	45.8 \pm 3.94	82.5 \pm 1.68	70.3 \pm 0.76	64.7 \pm 2.37	52.2 \pm 1.68
11		✓	Set 2	82.9 \pm 1.65	73.0 \pm 1.94	68.2 \pm 3.47	54.4 \pm 1.92	83.4 \pm 3.62	73.6 \pm 6.26	70.7 \pm 1.86	57.3 \pm 1.50
12		-	Set 2	85.8 \pm 1.70	75.3 \pm 0.39	69.0 \pm 2.53	54.6 \pm 2.09	87.8 \pm 1.33	78.2 \pm 1.02	70.0 \pm 2.55	58.3 \pm 1.61

Table A2: Results on PointGoalNav at 20 million. Same as Tab. 1 but at 20 million steps.

#	Sensors	Norm Adv.	HyperParams	SimpleCNN				ResNet18			
				Gibson		Matterport3D		Gibson		Matterport3D	
				Success \uparrow	SPL \uparrow	Success \uparrow	SPL \uparrow	Success \uparrow	SPL \uparrow	Success \uparrow	SPL \uparrow
1	RGB	✓	Set 1	57.8 \pm 6.23	43.8 \pm 3.43	07.6 \pm 3.00	06.2 \pm 2.39	68.2 \pm 2.87	52.7 \pm 2.87	41.4 \pm 1.61	30.1 \pm 1.10
2		-	Set 1	67.2 \pm 1.66	49.0 \pm 2.41	06.7 \pm 2.58	05.5 \pm 2.21	72.9 \pm 2.27	55.5 \pm 1.64	36.5 \pm 2.79	28.1 \pm 2.68
3		✓	Set 2	00.0 \pm 0.01	00.0 \pm 0.01	00.0 \pm 0.00	00.0 \pm 0.00	77.1 \pm 1.76	63.0 \pm 1.40	44.8 \pm 5.85	35.3 \pm 2.41
4		-	Set 2	72.6 \pm 1.32	53.6 \pm 2.27	21.5 \pm 5.32	15.4 \pm 3.02	77.0 \pm 1.11	62.9 \pm 1.24	38.9 \pm 1.53	32.6 \pm 0.95
5	RGB-D	✓	Set 1	76.6 \pm 1.06	64.9 \pm 0.56	53.3 \pm 2.86	39.5 \pm 1.81	84.2 \pm 1.27	75.6 \pm 1.08	66.2 \pm 3.17	52.6 \pm 1.28
6		-	Set 1	80.0 \pm 2.47	66.3 \pm 2.23	56.2 \pm 3.86	42.2 \pm 1.65	84.9 \pm 1.56	73.6 \pm 1.13	67.6 \pm 1.65	54.3 \pm 0.98
7		✓	Set 2	81.4 \pm 1.30	72.9 \pm 1.87	50.9 \pm 28.95	40.4 \pm 23.02	86.4 \pm 1.06	77.9 \pm 0.55	72.8 \pm 2.04	61.0 \pm 1.32
8		-	Set 2	84.4 \pm 0.85	73.0 \pm 1.07	66.6 \pm 2.77	51.6 \pm 2.00	86.5 \pm 0.85	78.0 \pm 0.42	72.2 \pm 1.74	60.5 \pm 0.77
9	Depth	✓	Set 1	79.8 \pm 1.41	71.0 \pm 1.60	64.7 \pm 1.92	51.1 \pm 1.73	86.6 \pm 1.02	77.6 \pm 2.42	70.4 \pm 2.99	57.2 \pm 2.09
10		-	Set 1	83.1 \pm 2.08	72.8 \pm 1.76	69.4 \pm 4.29	53.7 \pm 3.01	87.2 \pm 1.19	76.4 \pm 1.37	70.6 \pm 1.22	57.6 \pm 1.19
11		✓	Set 2	86.6 \pm 0.70	78.8 \pm 0.64	74.4 \pm 0.92	61.6 \pm 0.93	90.0 \pm 1.42	81.4 \pm 0.80	74.9 \pm 1.13	62.7 \pm 1.44
12		-	Set 2	90.2 \pm 1.63	80.6 \pm 1.13	73.7 \pm 2.66	60.0 \pm 1.59	90.8 \pm 0.96	81.1 \pm 1.18	72.7 \pm 1.76	62.1 \pm 1.70

Table A3: Results on PointGoalNav at 40 million. Same as Tab. 1 but at 40 million steps.

PPO Parameters	
PPO Epochs	4
PPO Mini-Batches	2
PPO Clip	0.2
Advantage normalization	No
γ	0.99
GAE- λ [45]	0.95
Learning rate	2.5×10^{-4}
Max gradient norm	0.5
Optimizer	Adam [53]
Number of Environemnts (NumSim)	6
Rollout length (RolloutLength)	128

Table A4: Base hyper-parameters (corresponds to hyper-parameter set 2 without normalized advantage). All experiments use these parameters unless state otherwise.